Large enhancement of macroscopic yield in attosecond pulse train–assisted harmonic generation

Mette B. Gaarde and Kenneth J. Schafer
Department of Physics and Astronomy, Louisiana State University, Baton Rouge, Louisiana 70803-4001, USA

Arne Heinrich, Jens Biegert, and Ursula Keller
ETH Zurich, Physics Department, Inst. of Quantum Electronics, CH-8093 Zürich, Switzerland
(Received 17 December 2004; published 28 July 2005)

Attosecond pulse trains (APT) are natural tools for controlling strong field processes, due to their periodicity and short duration. Here we present nonadiabatic calculations of the macroscopic harmonic signal created by a gas of helium atoms exposed to a strong infrared (IR) pulse in combination with an APT. We find that the harmonic yield can be enhanced by two to four orders of magnitude for the optimal delays between the IR and the APT pulses. The large enhancement is due to the change in the IR-intensity dependence of both the harmonic strength and phase caused by the presence and timing of the APT. This leads to enhancement of the harmonic yield and improved phase matching conditions over a large volume.

DOI: 10.1103/PhysRevA.72.013411 PACS number(s): 32.80.Qk, 42.65.Ky, 42.65.Re, 32.80.Wr

I. INTRODUCTION

It has recently been experimentally demonstrated that a train of pulses as short as a few hundred attoseconds is produced when several odd harmonics of an intense infrared (IR) laser field are combined in a phase-locked manner [1]. The short duration of the individual pulses in the train, and their periodicity which is half the fundamental IR cycle [2,3], make the attosecond pulse train (APT) an ideal tool to control strong field processes driven by the IR laser [4,5]. In [4] we considered high harmonic generation by a single helium atom, and used the timing of the APT relative to the IR pulse to select the time at which an electron is released into the continuum. Within the framework of the semiclassical model [6,7], this means that the APT can select which space-time trajectory the electron will follow in the continuum. We found that both the yield and the coherence properties of the harmonics were improved when the APT was timed to launch the electron along the shortest quantum path, which exhibits a slow phase dependence and therefore gives rise to well behaved harmonics [8].

In this paper we consider the harmonics generated by a macroscopic number of helium atoms exposed to the combination of a strong IR laser pulse and an APT, which are both represented by focused laser beams. We investigate whether the single atom effects of the APT can still be discerned after propagation and phase matching in the macroscopic nonlinear medium. Phase matching is in general imposed by a balance between the IR intensity dependence of the harmonic strength and phase, and the geometrical variations of the Guoy phase of the combined driving fields. In particular, we are interested in the following issues: (i) What is the consequence of the change in the relative phase over the spatial extent of the medium, imposed by the difference in carrier frequency (and thereby focusing characteristics) of the two pulses; and (ii) What is the interplay between the single atom quantum path selection imposed by the APT and the macroscopic quantum path selection imposed by phase matching?

To answer these questions we perform nonadiabatic calculations of the macroscopic harmonic response of a gas of helium atoms to the combined IR and APT focused laser pulses, by solving the Maxwell wave equation (MWE) coupled with the time-dependent Schrödinger equation (TDSE) (which is solved in the strong field approximation (SFA) [9]). We find that there are indeed phase matching conditions where the single atom quantum path selection has a very large impact on the generated harmonics. First, the choice of quantum path strongly influences the coherence properties of the macroscopic harmonics (for instance their spectral bandwidths), in agreement with the single atom results in [4]. Second, and more importantly, the harmonic yield can be enhanced by two to four orders of magnitude over most of the harmonic spectrum, for the optimal delays between the two driving pulses. This is a much larger enhancement than that of the single atom response. The large enhancement is due to the change in the IR intensity dependence of the harmonic strength and phase, caused by the presence and timing of the APT. At low IR intensity, the single atom enhancement of the harmonic signal is much larger than at high IR intensity. This means that atoms at the edge of the IR spatial profile contribute to the harmonic signal almost as much as atoms in the center of the IR beam, and we therefore achieve a large volume effect. In addition, phase matching is improved, since the harmonic phase varies much less with IR intensity when the APT is present. Finally, we discuss the validity of using the SFA as the single atom basis for our macroscopic calculation.

II. THEORETICAL METHOD

We solve the MWE in three dimensions in the slowly evolving wave approximation (SEWA), which is valid for pulses with durations as short as a single cycle (see Ref. [10] for details). We use an approach similar to that outlined in Ref. [11], in which the wave equation has the following form, in a coordinate system that moves with the driving pulse:

$$\nabla_{\perp}^2 \tilde{E}_D(\omega) + \frac{2i\omega}{c}\frac{\partial \tilde{E}_D(\omega)}{\partial z} = \tilde{G}(\omega) - \frac{i\omega}{c}\tilde{\alpha}(\omega)\tilde{E}_D(\omega), \quad (1)$$

$$\nabla_{\perp}^2 \tilde{E}_h(\omega) + \frac{2i\omega}{c}\frac{\partial \tilde{E}_h(\omega)}{\partial z} = -\omega^2 \mu_0 \tilde{P}_{nl}(\omega) + \tilde{G}(\omega) - \frac{i\omega}{c}\tilde{\alpha}(\omega)\tilde{E}_h(\omega), \quad (2)$$

where $\tilde{E}_D(\omega)$, $\tilde{G}(\omega)$, $\tilde{\alpha}(\omega)$, $\tilde{E}_h(\omega)$, and $\tilde{P}_{nl}(\omega)$ all are functions of the cylindrical coordinates r,z.

These equations are solved in the frequency domain, by space-marching all the frequency components of the driving field, $\tilde{E}_D(\omega)$, and the generated field $\tilde{E}_h(\omega)$, through the ionizing nonlinear medium. At each point z along the propagation direction, the temporal pulse shape of the driving field, $E_D(t)$, is found by Fourier transforming $\tilde{E}_D(\omega)$. The atomic response to the driving field $E_D(t)$ at each point in the radial direction is calculated in the time domain by solving the TDSE, as described below. This yields the time-dependent dipole moment $d_{nl}(t)$ and the free electron density $n_e(t)$. The source terms $\tilde{G}(\omega)$ (owing to free electron dispersion) and $\tilde{P}_{nl}(\omega)$ (the nonlinear polarization) are then found by transforming back into the frequency domain ($\tilde{F}$):

$$\tilde{G}(\omega) = \tilde{F}\left[\frac{e^2 n_e(t)}{\epsilon_0 m_e c^2} E_D(t)\right], \quad (3)$$

$$\tilde{P}_{nl}(\omega) = \tilde{F}\{[n_0 - n_e(t)]d_{nl}(t)\}, \quad (4)$$

and are used to propagate all the electric fields forward in z. n_0 is the initial gas density. Absorption is included for all frequencies above the ionization threshold of helium, using the absorption coefficients $\tilde{\alpha}(\omega)$ of Ref. [12]. The absorption coefficient is proportional to the density of neutral atoms.

For this study, we have calculated the free electron density from ionization rates calculated as described by Ammosov, Delone, and Krainov (ADK) [13], and we use the SFA to calculate the time-dependent dipole moment [9], in a nonadiabatic form as in Eq. (1) of Ref. [11]. In this description, the time-dependent dipole moment is an integral over quantum trajectories that each corresponds to an electron which is released into the continuum at time t', accelerates in the laser field, and returns to the core at a later time t. During the continuum propagation the electron acquires a phase given by the quasiclassical action, $S(t',t)$. Only trajectories that correspond to stationary points of the action are included. When calculating these stationary points, $S_{st}(t',t)$, we perform an additional approximation and use a vector potential $A_{IR}(t)$ which does not include contributions from the APT:

$$S_{st}(t',t) = (t-t')I_p - \frac{1}{2}p_{st}^2(t',t)(t-t') + \frac{1}{2}\int_{t'}^{t} A_{IR}^2(t'')dt''. \quad (5)$$

In this equation I_p is the atomic ionization potential and the stationary value of the momentum $p_{st}(t',t)$ is given by

$$p_{st}(t',t) = \frac{1}{t-t'}\int_{t'}^{t} A_{IR}(t'')dt''. \quad (6)$$

Neglecting the influence of the APT during the continuum propagation is consistent with the interpretation presented in Ref. [4] for the strong field dynamics in the combined IR and APT fields: the ionization step is dominated by one photon ionization driven by the APT, and the continuum dynamics are controlled by the IR field, whose ponderomotive energy is several orders of magnitude larger than that of the APT. Discarding the APT in the calculation of the saddle points also gives single atom results in better agreement with the results of the full numerical solution to the TDSE [4]. In the propagation code, $A_{IR}(t)$ is calculated as the Fourier transform of the product of the combined propagating driving field $\tilde{E}_D(\omega)$ and a spectral window function which suppresses the high frequency components. The Fourier transform of the full $\tilde{E}_D(\omega)$ is used in the SFA for the ionization step, and to calculate the ADK ionization rates.

The driving field at the entrance to the medium is the sum of an 810 nm IR pulse with a peak intensity of a few times 10^{14} W/cm^2 and an APT with a peak intensity of 10^{13} W/cm^2. The train consists of the odd harmonics 11 through 19 of the IR field. The envelope of the IR intensity is a $\cos^4$ function with a full width at half maximum (FWHM) duration of 27 fs, and the envelope of the APT is the fourth power of the driving field envelope and has a FWHM duration of 14 fs. At the entrance to the non-linear medium, the IR and the APT are described by Gaussian beams with confocal parameters b_{IR}=0.5 cm and b_{XUV}=7.5 cm, respectively. The position of the focus of each beam relative to the center of the gas jet can be chosen independently. In all the calculations shown below, the focus of the APT has been kept at the center of the medium. The factor of 15 difference in the confocal parameters is chosen to ensure that the waists of the two beams are similar (about 25 μm) over the 0.1 cm length of the medium. This maximizes the volume of atoms that experience the combined fields. The relative phases of the harmonics in the train are chosen so that, in the absence of dispersion effects, the harmonics are exactly phase locked in the focus of the XUV beam, and slightly out of phase at the beginning and at the end of the medium.

In a typical calculation, we use 8000 points in time and frequency, 301 points in the radial direction (spanning 100 μm), and 251 points in the propagation direction (spanning the length of the medium, 0.1 cm). For the choice of parameters in this study, it is only necessary to evaluate the source terms approximately every 10 steps in the z direction (as was also noted in Ref. [11]). To further speed up the calculation, we use perturbation theory to calculate the harmonic response at the lowest intensities.

III. RESULTS

Figure 1 presents macroscopic harmonic spectra generated in a 0.1 cm long jet of helium atoms with a density of 2×10^{18} atoms/cm^3 (which corresponds to 60 Torr at room temperature), when the IR laser beam is focused 0.2 cm be-

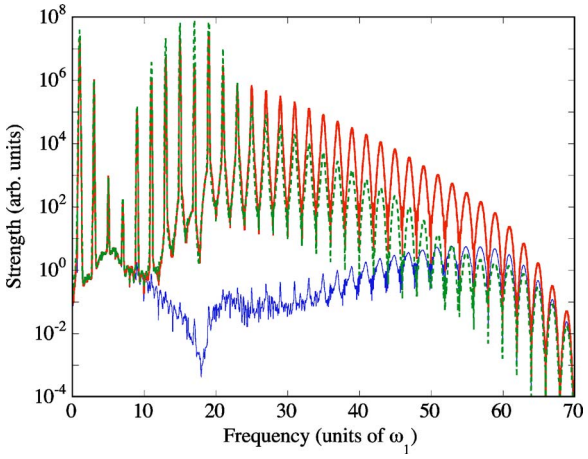

FIG. 1. (Color online) Harmonic spectra generated by a 5×10^{14} W/cm^2 IR pulse alone (thin solid line), or in combination with a 10^{13} W/cm^2 attosecond pulse train, for two different values of the delay between the two pulses. The delays are, in units of the IR cycle, $t_d=-0.095$ (thick solid line) and $t_d=+0.185$ (dashed line). The confocal parameters of the IR and the XUV beams are 0.5 cm and 7.5 cm, respectively. The IR focus is located 0.2 cm before the center of the 0.1 cm gas jet, the XUV focus is in the center of the jet.

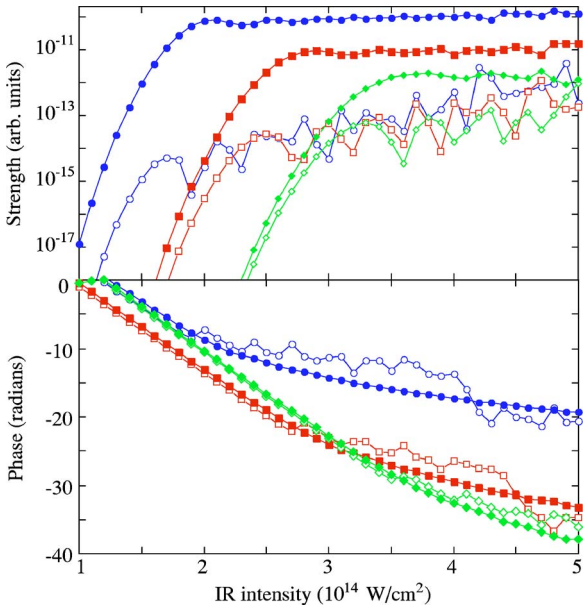

FIG. 2. (Color online) Comparison of the IR intensity dependence of the single atom harmonic strength and phase, when the harmonics are calculated with the IR pulse alone (open symbols), or in combination with a 10^{13} W/cm^2 APT (filled symbols). We show three harmonics, the 39th (circles), the 49th (squares), and the 59th (diamonds). The calculations were performed within the SFA.

fore the center of the jet ($z_{IR}=0.2$ cm). In this focus position, the phase matching conditions favor the contributions from the short quantum trajectory (see for instance Refs. [3,8]). This can be seen from the spectral widths of the harmonics generated by the IR pulse alone (thin solid curve), which are small in the plateau region and increase with the harmonic order.

The thick solid line shows the spectrum generated by the combined IR and APT pulses, when the relative delay between the two pulses, in the center of the medium, is −0.095. The delay is measured in units of the IR optical cycle, and $t_d=0$ means that the attosecond pulses in the train coincide with the zero crossing of the electric field in each half-cycle. The delay $t_d=-0.095$ was found to be optimal for quantum path selection of the short trajectory contribution in single atom calculations based on numerical integration of the time-dependent Schrödinger equation within the single active electron (SAE) approximation [4]. The SFA single atom calculations reproduce this result. The effect of the APT pulse on the macroscopic signal is a very large enhancement over most of the spectral range. The harmonics between 39 and 51 (with photon energies from 60–80 eV), for instance, are enhanced by three to four orders of magnitude. The shape of the spectrum is also significantly different with its constant decrease as the photon energy increases. The bandwidths of the individual harmonics are still characteristic of the short trajectory contribution.

The origin of the large enhancement seen in Fig. 1 is illustrated in Fig. 2, showing the single atom strength (a) and phase (b) for harmonics 39 (circles), 49 (squares), and 59 (diamonds) as the peak intensity of the IR pulse varies between 1 and 5×10^{14} W/cm^2. We compare the strength and phase generated by the IR pulse alone (open symbols) with that generated in combination with the APT (closed symbols). Each point is the result of a single atom calculation with a 27 fs IR pulse with a different IR peak intensity, and the same APT peak intensity of 10^{13} W/cm^2. This is justified because the harmonic strength varies only linearly with the APT intensity, as opposed to its nonlinear dependence on the IR intensity. The harmonic phase also varies slowly with APT intensity [4].

The APT has several effects on both the strength and the phase of the harmonics. First, the harmonics up to approximately the 59th are all enhanced by several orders of magnitude, for all intensities below the peak intensity used in the macroscopic calculation. Second, the enhancement is in general much larger at low intensity than at high intensity—the strength is essentially flat as a function of intensity once a harmonic has reached the plateau. This means that atoms at the edge of the IR radial profile, which in the absence of the APT contribute very little to the macroscopic signal, now contribute to the harmonic signal as much as atoms in the center of the IR beam. We therefore get a large volume effect that contributes to the enhancement of the total macroscopic signal. To achieve this volume effect it is very important that the IR and the APT beams overlap in the radial dimension through most of the medium, which necessitates the much longer confocal parameter of the APT beam. Third, the enhancement is in general larger for the lower harmonics than for the higher harmonics. This gives rise to the altered shape of the two-color spectrum, with the strength decreasing as a function of the harmonic order. And finally, the characteristic quantum path interference, which in the IR alone calculations gives rise to the rapid variation of the harmonic strength with the IR intensity, vanishes when the APT is present. This is consistent with the interpretation that the

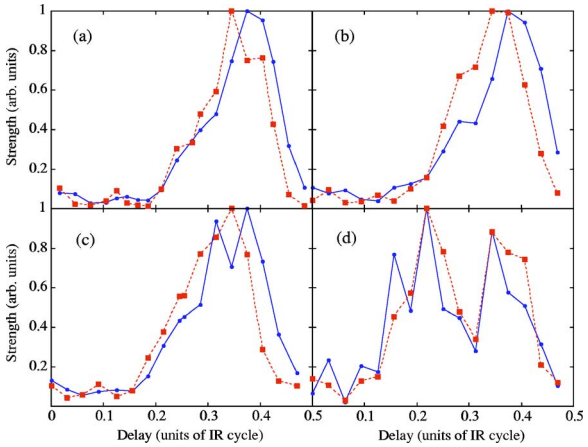

FIG. 3. (Color online) The delay dependence of the 43rd and the 53rd harmonics, shown with circles and squares, respectively, driven by the combined IR and APT pulses. In (a) and (c) we show the yield after propagation through a 1 mm gas jet, for two different positions of the IR focus, $z_{IR}=-0.2$ cm (a) and $z_{IR}=0$ (c). The atomic density is 4×10^{17} per cm^3. All other parameters are as in Fig. 1. In (b) and (d) we show the single atom yields, calculated with the SFA (b), and with the SAE (d), using peak intensities of 4×10^{14} W/cm^2 for the IR and 10^{13} W/cm^2 for the APT.

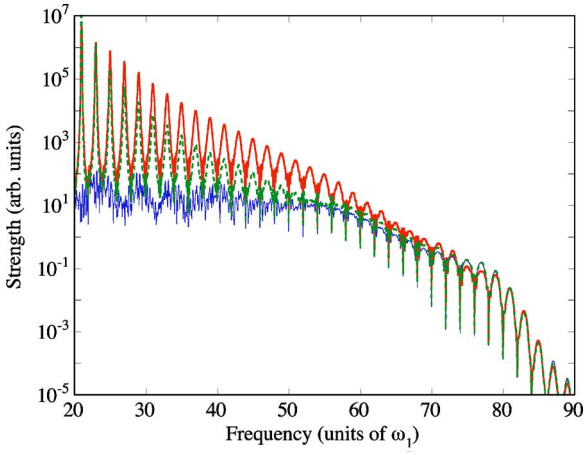

FIG. 4. (Color online) Harmonic spectra generated by a 5×10^{14} W/cm^2 IR pulse alone (thin solid line), or in combination with a 10^{13} W/cm^2 attosecond pulse train, for two different values of the delay between the two pulses. The delays are, in units of the IR cycle, $t_d=-0.094$ (thick solid line) and $t_d=+0.125$ (dashed line). The confocal parameters of the IR and the XUV beams are 0.5 cm and 7.5 cm, respectively. Both beams are focused in the center of the gas jet.

APT selects one quantum path out of several. This absence of interference is also clear in the intensity dependent phase which becomes smoother and flatter when the APT is present. Phase matching is thus also improved by the presence of the APT.

The single atom enhancement of the harmonic strength is a result of two effects, both of which can be discussed within the framework of the semiclassical model of harmonic generation. First, the initial ground state to continuum transition is a one photon process for the APT but a multiphoton process for the IR. And second, the timing of the electron's release into the continuum with the natural release time for the short trajectory means that the electron is much more likely to return to the core, compared to when it is released throughout the cycle as in tunneling ionization. The first of these effects is delay independent and could be achieved by a pulse consisting of just one harmonic of the IR field, whereas the second effect depends on the delay between the two pulses and relies on the short duration of the individual attosecond pulses in the train.

That the relative delay indeed matters for the macroscopic harmonic signal can be seen from the dashed curve in Fig. 1. This has been calculated with a delay of $t_d=+0.185$, at which there is no quantum path selection in the SFA. The enhancement is now much smaller than at $t_d=-0.095$, and at the end of the plateau there is no enhancement compared to the IR alone result. There is, however, still a substantial enhancement of the harmonics between 30 and 50 [14]. We believe this is mostly driven by the single atom enhancement and the resulting volume effect discussed in the previous paragraph.

Figure 3(a) explores in more detail the delay dependence of the macroscopic yield of harmonics 43 and 53 generated in the phase matching conditions used in Fig. 1 [15], but at a lower atomic density (4×10^{17} per cm^3). The yields have been normalized for comparison. The harmonics from approximately 35 to 63 all exhibit similar behavior with respect to the delay. The yield for each harmonic varies by more than an order of magnitude as the delay is changed, and is strongly peaked for delays between 0.35 and 0.4 (or −0.15 and −0.1). The higher harmonics are peaked at earlier delays than the lower harmonics, and exhibit more structure as the delay varies.

The variation with delay originates in the single atom delay dependence, as shown in Fig. 3(b). We show the same two harmonics, calculated within the SFA. The position of the peak at $t_d\approx-0.1$ (or 0.4 in the figure) can be explained using the analysis of Ref. [4]. The electrons released by the APT in general have a small initial velocity. If the electron released close to −0.1 initially moves downhill with respect to the laser potential, it can return to the core only by following the short quantum path. It is characteristic of the short trajectory that the return energy increases when the electron is released earlier and returns later. This leads to the shift of the optimum delay for the higher harmonics compared to the lower ones. The width of the enhancement peak is comparable to the 270 as duration of the individual pulses in the APT.

Next we explore the influence of the phase matching conditions on the two-color harmonic generation. Figure 4 shows a macroscopic harmonic spectrum calculated with the same parameters as in Fig. 1 except the position of the IR laser focus, which is now in the center of the gas jet. At this position of the focus, the phase matching conditions favor contributions from the longer quantum paths. This causes the spectral bandwidths of neighboring harmonics to spread and overlap, as can be seen in the IR alone curve (thin solid line). The spectrum generated by the IR in combination with the APT, with a relative delay of $t_d=-0.095$, is shown with thick solid line. The presence of the APT in this case both en-

hances the harmonic yield and changes the spectral structure of the individual harmonics due to the quantum path selection of the short trajectory contribution. The APT is thus able to impose a different kind of phase matching on the generated harmonics. The dashed line shows the result of a relative delay of $t_d=+0.125$. The enhancement at this delay is much lower, between one and two orders of magnitude. The highest harmonics (between 50 and 65) are barely enhanced at $t_d=+0.125$, and their spectra are broad and noisy.

The dependence of the yield on the delay when $z_{IR}=0$ is very similar to the dependence found for $z_{IR}=-0.2$ cm, as is shown in Fig. 3(c). The macroscopic variation of the yield again closely reflects the single atom behavior, both with respect to the position of the peak enhancement, and the difference between good delays and bad delays. It is interesting how relatively little the position of the IR focus relative to the gas jet matters when the APT is present, which is in stark contrast to macroscopic harmonic generation driven by an IR pulse alone. The changes in the harmonic strength and phase driven by the quantum path selection of the APT apparently dominate the build-up of the harmonic radiation in the macroscopic medium. However, it is clear from the difference in the enhancement between Figs. 1 and 4 that the influence of the quantum path selection is highest when the phase matching conditions work together with it (as in Fig. 1) rather than against it (Fig. 4).

In the phase matching configurations discussed in this paper, the number of photons generated in each harmonic in the IR alone case is low. This is because of the short IR confocal parameter (0.5 cm) and the short medium length (and the intensity, of course, which is far below the saturation intensity of 10^{15} W/cm^2). The IR spectrum in Fig. 1 for instance only corresponds to a few tens of photons per pulse in each of the harmonics between 35 and 55. With the large enhancement of the APT (top spectrum in Fig. 1), we get more than 10^5 photons in the 35th harmonic, 10^4 photons in the 45th harmonic, and 10^3 photons in the 55th harmonic. Since the enhancement comes from the spatial overlap between the two beams, or in particular from the region where the APT is strong, it scales well with an increase of the interaction region. Increasing the confocal parameters of both beams, as well as the length of the gas jet, by a factor of 2 gives almost an order of magnitude increase in the number of photons generated both in the IR alone and in the two beam case. In the calculation, the only limitation to keep increasing the interaction region is the absorption of the 17th and 19th harmonics which are just above the ionization threshold in the field-free helium atom. We note, though, that we are using the field-free values for the absorption cross section in helium, i.e., the calculation does not take into account dynamical effects (such as ac Stark shifts) arising from the interaction of the atom with the strong IR field. Increasing the IR intensity would somewhat increase the number of photons in the IR alone case, but only marginally increase the number of photons in the two color case. This is because the enhancement driven by the APT strongly depends on the initial ionization step being driven by the APT. If the IR intensity is increased to the point where it dominates the ionization step, the enhancement (and the quantum path selection) is no longer dominant.

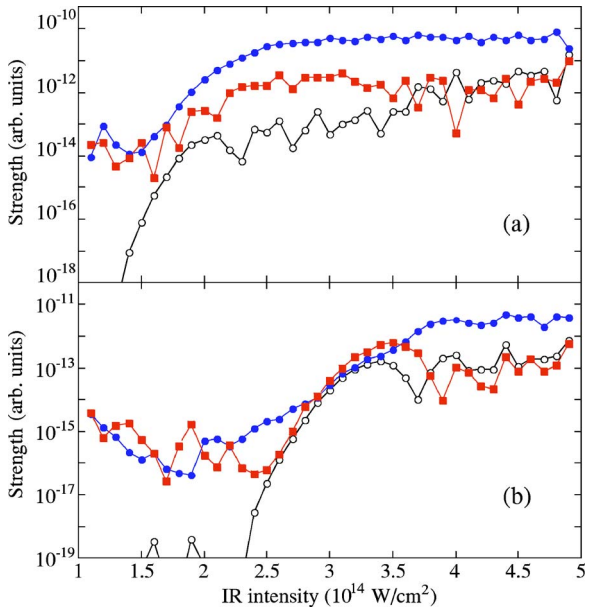

FIG. 5. (Color online) IR intensity dependence of the single atom strength of harmonics 43 (a) and 59 (b), calculated by numerical integration of the TDSE within the SAE approximation, for two different delays between the IR and the APT pulses. The delays are, in units of IR cycles, $t_d=-0.094$ where the short trajectory is selected (filled circles) and $t_d=+0.063$ where no trajectories with returns within one cycle are selected (filled squares). The strength of the harmonics driven by the IR pulse alone is shown with open circles.

Finally, we discuss the validity of using ADK rates and the SFA as the single atom basis for the macroscopic calculation. First, the ionization rates are only used to calculate the number of free electrons in the medium and thereby the refractive index (the harmonic strength is calculated within the SFA). In the macroscopic conditions where we expect to see the enhancement by the APT, the electron density is very low due to both the low atomic density and ionization yields of a few percent at most, as discussed in the previous paragraph. The refractive index therefore plays a very small role in the propagation of the fundamental. In addition, the ADK ionization rates, which are based on a tunneling ionization picture, underestimate the ionization caused by the APT but overestimate the ionization caused by the IR for intensities above 3×10^{14} W/cm^2. The ionization yields predicted by the ADK rates in our conditions are therefore overall in good agreement with those of a more accurate calculation [4]. Second, for comparison with the SFA results shown in Fig. 2(a), Fig. 5 shows the single atom intensity dependence of harmonics 43 (a) and 59 (b) calculated by direct numerical integration of the TDSE within the SAE approximation [16,17]. The APT pulse has a duration of 14 fs and a peak intensity of 10^{13} W/cm^2, and the IR pulse has a duration of 27 fs and a peak intensity which varies up to 5×10^{14} W/cm^2. We show two different delays, $t_d=-0.094$, where the short trajectory is selected (filled circles), and $t_d=+0.063$ where no trajectories are selected by the APT (squares). We also show the dependence on the IR intensity in the absence of the APT (open circles).

In Fig. 5, the magnitude of the enhancement at $t_d = -0.094$ is similar to, though marginally smaller than, that found with the SFA (Fig. 2). Also the larger enhancement at low intensity, the larger enhancement of the lower harmonics than the higher harmonics, and the absence of interference in the intensity dependence, are correctly reproduced by the SFA (Fig. 2) compared to the full calculation (Fig. 5) [18]. The SAE also predicts, like the SFA, that there is some enhancement of the lower order harmonics even at delays where no trajectories are selected (at least no trajectories that return within one cycle of the field), as seen from the $t_d = +0.063$ curves.

We therefore expect the macroscopic calculations based on the SFA to approximately predict the outcome of an experiment, in terms of the enhancement of the yield and the change in the spectral characteristics of the harmonics, when the delay between the IR and the APT is chosen to select the short quantum path. However, in one respect we do expect an experiment to differ from the result presented in Figs. 3(a) and 3(c), namely in the dependence on the relative delay. Figure 3(d) shows the single atom yield calculated within the SAE as a function of the relative delay. In addition to the peak in the yield around $t_d = 0.4$ (or $t_d = -0.1$) there is clearly a second, equally strong, peak centered around $t_d = 0.25$. This peak corresponds to electrons that are released and initially move *uphill* with respect to the potential, before scattering on the core and then being accelerated in the characteristic short trajectory manner [4]. This second peak is absent in the SFA prediction.

We attribute the origin of this discrepancy to the simplified description of the ground state to continuum transition in the SFA compared to the SAE, and the absence of the atomic potential once the electron is in the continuum. In the SAE calculations, the electron that is ionized by the APT is released with a small, delay-dependent initial velocity, and its motion close to the core depends on the details of the combined atomic and laser potential. In contrast, in the SFA the saddle point trajectories correspond to electrons released with zero initial velocity. These electrons can only move downhill in the laser potential and we therefore do not see the quantum path selection corresponding to the uphill electron. In an experiment, we thus expect to see an enhancement vs delay curve that looks like that in Fig. 3(d), rather than Fig. 3(a).

IV. SUMMARY

We have studied harmonic generation by a macroscopic number of helium atoms interacting with a combination of a strong IR laser pulse and an attosecond pulse train. We have shown that the yield of many harmonics can be simultaneously enhanced by several orders of magnitude compared to the IR alone case, when the timing of the APT is such that the shortest quantum trajectory is selected. In this case the spectra of the individual harmonics are well resolved, independent of the phase matching conditions. The large enhancement is due to the change in the IR intensity dependence of the harmonic strength and phase caused by the presence of the APT. In particular, the enhancement is much larger at low IR intensity than at high IR intensity. This means that atoms at the edge of the IR radial profile, which in the absence of the APT contribute little to the harmonic signal, contribute significantly to the macroscopic harmonic signal. We therefore achieve a large volume effect. Phase matching in the macroscopic medium thus not only permits the observation of the single atom quantum path selection driven by the timing of the APT, but actually enhances its effects.

Finally, we have compared our SFA single atom results to the more accurate results calculated within the SAE, and identified a range of conditions where we expect our SFA based predictions to be valid. The missing uphill electron trajectory in the SFA, and the overestimation of the enhancement of harmonics below approximately the 30th, indicates the need for large scale nonadiabatic MWE-TDSE solvers that incorporate more accurate solutions of the Schrödinger equation into the propagation [19].

ACKNOWLEDGMENTS

M.G. acknowledges the support from the Louisiana Board of Regents through Grant No. LEQSF(2004-07)-RD-A-09. K.S acknowledges the support from the National Science Foundation through Grant No. PHY-0401625.

[1] P. M. Paul *et al.*, Science **292**, 1689 (2001).
[2] S. Harris, J. J. Macklin, and T. W. Häansch, Opt. Commun. **100**, 487 (1993);and G. Farkas and C. Toth, Phys. Lett. A **168**, 447 (1992).
[3] Ph. Antoine, A. L'Huillier, and M. Lewenstein, Phys. Rev. Lett. **77**, 1234 (1996).
[4] K. J. Schafer, M. B. Gaarde, A. Heinrich, J. Biegert, and U. Keller, Phys. Rev. Lett. **92**, 023003 (2004).
[5] P. Antoine *et al.*, in *Proceedings of the 7th International Conference on Multiphoton Processes*, edited by P. Lambropoulos and H. Walther (Institute of Physics Publishing, Bristol, 1996).
[6] K. J. Schafer, B. Yang, L. F. DiMauro, and K. C. Kulander, Phys. Rev. Lett. **70**, 1599 (1993).
[7] P. B. Corkum, Phys. Rev. Lett. **71**, 1994 (1993).
[8] M. Bellini, C. Lyngå, A. Tozzi, M. B. Gaarde, T. W. Hänsch, A. L'Huillier, and C.-G. Wahlström, Phys. Rev. Lett. **81**, 297 (1998).
[9] M. Lewenstein, Ph. Balcou, M. Yu. Ivanov, A. L'Huillier, and P. B. Corkum, Phys. Rev. A **49**, 2117 (1994).
[10] T. Brabec and F. Krausz, Rev. Mod. Phys. **72**, 545 (2000).
[11] E. Priori, G. Cerullo, M. Nisoli, S. Stagira, S. De Silvestri, P. Villoresi, L. Poletto, P. Ceccherini, C. Altucci, R. Bruzzese, and C. de Lisio, Phys. Rev. A **61**, 063801 (2000).
[12] B. L. Henke, E. M. Gullikson, and J. C. Davis, At. Data Nucl.

Data Tables **54**, 181 (1993).
[13] M. V. Ammosov, N. B. Delone, and V. P. Krainov, Zh. Eksp. Teor. Fiz. **91**, 2008 (1986) [Sov. Phys. JETP **64**, 1191 (1986)].
[14] The SFA prediction for the harmonics below approximately 30 ω_1 is much higher than the SAE prediction, and we therefore in general do not discuss results for those harmonics in this paper.
[15] In the calculation, the delay was varied between −0.25 and 0.25. For clarity, delays between −0.25 and 0 have been shifted by one half IR cycle are shown as varying from 0.25 to 0.5 in the plot.
[16] K. C. Kulander, K. J. Schafer, and J. L. Krause, in *Atoms in Intense Laser Fields*, edited by M. Gavrila (Academic Press, San Diego, 1992).
[17] K. J. Schafer and K. C. Kulander, Phys. Rev. Lett. **78**, 638 (1997).
[18] The large enhancement of the harmonics at the lowest intensities compared to the IR alone yield is only a result of increased noise when the APT is present.
[19] N. H. Shon, A. Suda, and K. Midorikawa, Phys. Rev. A **62**, 023801 (2000).